



ELSEVIER

Biophysical Chemistry 77 (1999) 79–97

Biophysical  
Chemistry

# Observations on the origin of the non-linear van't Hoff behaviour of polypeptides in hydrophobic environments

Reinhard I. Boysen, Yeqiu Wang, Hooi Hong Keah, Milton T.W. Hearn\*

*Centre for Bioprocess Technology, Department of Biochemistry and Molecular Biology, Monash University, Clayton, Victoria, Australia 3168*

Received 17 August 1998; received in revised form 4 December 1998; accepted 28 December 1998

## Abstract

In this paper we describe a general procedure to determine the thermodynamic parameters associated with the interaction of polypeptides or proteins with immobilised lipophilic compounds such as non-polar *n*-octyl groups. To this end, the binding behaviour of an all L- $\alpha$ -polypeptide, **1**, and its retro-inverso-isomer, **2**, has been investigated with an *n*-octylsilica and water–organic solvent mixture containing different percentages of acetonitrile or methanol over the temperature range of 278–338 K. The results confirm that non-linear van't Hoff plots occur with this pair of polypeptide isomers, depending on the solvent composition. These findings are consistent with the changes in the thermodynamic parameters, enthalpy of association,  $\Delta H_{assoc,i}^o$ , entropy of association,  $\Delta S_{assoc,i}^o$ , and heat capacity,  $\Delta C_{p,i}^o$ , all having significant temperature dependencies. Theoretical relationships linking the changes in the  $\Delta H_{assoc,i}^o$ ,  $\Delta S_{assoc,i}^o$  and  $\Delta C_{p,i}^o$  values of these polypeptide–non-polar ligate systems, as a function of temperature, *T*, have been validated. Significant differences were observed in the magnitudes of these thermodynamic quantities when acetonitrile or methanol was employed as the organic solvent. The origin of these solvent-dependent effects can be attributed to the hydrogen-bonding propensity of the respective solvent. Involvement of enthalpy–entropy compensation effects associated with the interaction of these polypeptides with the hydrophobic ligates has also been documented. Analysis of empirical extra-thermodynamic relationships associated with molecular structural properties of these polypeptides, such as the slope term, *S*, derived from the plots of the logarithmic capacity factor,  $\log k'_i$ , of these polypeptides vs. the volume fraction of the organic solvent,  $\phi$ , as a function of temperature, *T*, has also revealed similar correlations in terms of the interactive behaviour of polypeptides **1** and **2** under these experimental conditions. These findings provide an extended thermodynamic and extra-thermodynamic framework to examine the solvational, conformational and other equilibrium processes that polypeptides (or proteins) can undergo in the presence of *n*-alkylsilicas or other classes of immobilised hydrophobic surfaces. The experimental approach utilised in this study with these topologically similar polypeptides thus represents a generic procedure to explore the behaviour of polypeptides or proteins in non-polar environments in terms of their molecular properties and the associated linear free energy relationships that determine their interactive behaviour. © 1999 Elsevier Science B.V. All rights reserved.

**Keywords:** Peptide isomers; Lipophilic binding; Thermodynamics; Non-linear van't Hoff plots; Temperature effects; Solvent effects

\*Corresponding author. Tel.: +61 3 99053720; fax: +61 3 99055882; e-mail: milton.hearn@med.monash.edu.au

## 1. Introduction

Over the past two decades, high performance liquid chromatographic (HPLC) methods, and reversed phase HPLC (RP-HPLC) procedures in particular, have become indispensable techniques for the analysis of peptides and proteins as part of biochemical and biological investigations [1,2]. Furthermore, with RP-HPLC procedures, it is now feasible to examine the molecular nature of the characteristic interconversion of the secondary and tertiary structures that polypeptides and proteins can undergo when they interact with immobilised *n*-alkyl ligands or other classes of hydrophobic ligands in the presence of aquo-organic solvent environments [3–5]. As such, RP-HPLC procedures provide a very useful experimental avenue to explore the role of the hydrophobic effect in the conformational stabilisation of polypeptides and proteins in heterogeneous lipophilic systems. Because of this potential, RP-HPLC procedures, as well as the other interactive modes of HPLC, such as high performance ion exchange chromatography (HPIEX), high performance hydrophobic interaction chromatography (HPHIC) and high performance immobilised metal ion affinity chromatography (HPIMAC), represent more than just a powerful set of separation tools. These methods also provide versatile experimental opportunities to derive information on the biophysical behaviour of biomacromolecules at solvated chemical surfaces, as models of their behaviour in biological systems. Studies on the dependence of the free energy related retention/binding parameters upon the experimental conditions thus provides an avenue to elaborate the nature of the physico-chemical factors and molecular descriptor terms that are associated with the interactive process(es) occurring between a polypeptide (the ligand) and immobilised binding groups (the ligates).

These dependencies have, in the past, been frequently evaluated only in terms of empirical relationships, such as the linearised plots of the logarithmic retention factor,  $\log k'_i$ , of a polypeptide (or protein),  $P_i$ , vs. the mole fraction,  $c_i$ , or volume fraction,  $\varphi_i$ , of the displacing solvent or other chemical species [6]. The slopes of these

linearised dependencies, referred to as the *S*-values [1,7] in the case of the reversed phase mode of interaction, i.e.  $\log k'_i = \log k_{o,i} - S\varphi_i$ ; the *H*-value [8] in the case of the hydrophobic interaction mode; the *Z*-value [9,10] in the case of the ion exchange mode; or the *M*-value [11] in the case of the immobilised metal ion affinity mode, as well as the extrapolated *y*-intercept values of these linearised plots when  $c_i \rightarrow 0$  or  $\varphi_i \rightarrow 0$ , i.e. the corresponding  $\log k_{o,i}$ -values, can then be interpreted in terms of linear free energy relationships (LFERs) or other steric/molar/structural terms that characterise the molecular properties of ligand–ligate interactions.

When lipophilic compounds are immobilised onto a support material such as a porous silica, the magnitude of the measured *S* (and the corresponding  $\log k_{o,i}$ ) term of an individual polypeptide or protein, together with their kinetic behaviour as manifested by the bandwidth changes of the peak profile, can be used to reveal information on the effect of amino acid sequence substitutions, the consequences of L- $\alpha \rightarrow$  D- $\alpha$ -amino acid racemisation, and also the effect of changes in the secondary (or tertiary) structure of these biosolutes that are induced by the perturbing, dynamic conditions associated with the interaction with the solvated *n*-alkyl ligates [1,11–16]. In previous investigations with low molecular weight organic compounds and various biomacromolecules, the ‘near-equilibrium’ criterion of binding and desorption behaviour has generally been assumed. As a consequence, changes in the thermodynamic parameters of the ligand–ligate interaction can be depicted in terms of criteria specified by the Gibbs–Helmholtz relationship, namely:

$$\Delta G_{assoc,i}^o = \Delta H_{assoc,i}^o - T\Delta S_{assoc,i}^o \quad (1)$$

Under such binding conditions, the properties of the solute, the surrounding bulk and structures solvent and the interactive surface have in many previous investigations been assumed to be invariant with regard to the temperature, *T*, and hence the contributions from the corresponding changes in enthalpy,  $\Delta H_{assoc,i}^o$ , or entropy,  $\Delta S_{assoc,i}^o$ , to the overall Gibbs free energy change,

$\Delta G_{assoc,i}^o$ , associated with the solute–sorber interaction, as well as the phase ratio of the system,  $\Phi$ , will also be independent of temperature. When such conditions prevail, then the dependency of  $\log k'_i$  on  $1/T$  takes the form of the well-known linear van't Hoff plot. Although this behaviour has been observed experimentally in several cases with small peptides [1,11,13–16], in an increasing number of investigations with polypeptides and proteins studied under such conditions significant divergencies from this ideal behaviour have been observed [1,11,17–20]. In the present investigation, the thermodynamic and extra-thermodynamic basis of this non-linear van't Hoff behaviour when polypeptides interact with lipophilic ligates in aquo-organic solvent environments has been examined more closely. In particular, the influences of temperature and solvent composition on the interactive behaviour of a topologically related polypeptide pair, the all L- $\alpha$ -DDALYD-DKNWDRAPQRCYYQ, **1**, and the all D- $\alpha$ -QYYCRQ-PARDWNKDDYLADD, **2**, respectively, have been examined.

Retro-inverso-enantiomeric polypeptide pairs with the structural features of the polypeptide 20-mers, **1** and **2**, represent a special class of compounds with the characteristic that they can assume similar  $\phi/\psi$  dihedral angles along the polypeptide backbone, and thus, in principle, can adopt similar conformations in solution, despite the complete reversal of their amino acid sequences [21,22]. Besides offering an avenue to examine fundamental questions about the nature of the hydrophobic effect and its role in the interaction and folding of polypeptides in the presence of polar or lipophilic ligates per se, a further motivation for the use of retro-inverso-enantiomeric polypeptides, particularly those related to peptide hormones, anti-microbial peptides, peptide-subunit vaccines or peptide neurotransmitters [23–26] has been the desire to improve the biological properties of agonist/antagonist analogues, including increased resistance to proteolytic degradation, enhancement of the affinity of the analogue for its appropriate biological acceptor/receptor and improved transmembrane transport. Moreover, with retro-inverso-enantiomeric polypeptides (and the corre-

sponding enantiomeric or retro-enantiomeric polypeptide pairs) the stereo-electronic contributions that specific amino acid side chains make to a particular ligand–acceptor interaction can be assessed.

Such topological approaches date back over 30 years to the pioneering studies with enantio-an-niatin A/B and retro-enantio-gramicidin S [27,28]. Subsequently, other studies have examined the biological properties of various L- $\alpha$ -/D- $\alpha$ -peptide enantiomeric pairs (reviewed Goodman and Chorev [21,22,29]). Generally, L  $\rightarrow$  D substitutions have been employed either as a direct replacement strategy without reversal of the direction of the sequence, thus generating peptide pairs which are enantiomerically related, such as the [Gly<sup>5</sup>,Gly<sup>10</sup>]gramicidin S/retro-enantio-[Gly<sup>5</sup>,Gly<sup>10</sup>]gramicidin S [28] or melittin/retro-enantio-melittin [30], or alternatively with inversion of the sequence developing an all D- $\alpha$ -peptide which notionally has topological equivalence with the corresponding all L- $\alpha$ -peptide, such as the peptide pairs bradykinin/retro-inverso-bradykinin, the major antigenic site of foot and mouth disease virus FMDV-VP1<sup>141-159</sup>/retro-enantio-FMDV-VP1<sup>141-159</sup> [31] or the all L- $\alpha$ -, all D- $\alpha$ - and retro-inverso-analogues of model hexapeptide sequences corresponding to the C-terminal region of histone H3 [32].

Surprisingly, very few investigations have been reported on the biophysical behaviour of all L- $\alpha$ -/all D- $\alpha$ -retro-inverso-isomer polypeptide pairs at polar and/or non-polar interfaces or their solution conformational properties. Amongst the few comparative studies on the structure–activity relationships of all L- $\alpha$ -/all D- $\alpha$ -retro-inverso peptide pairs, <sup>1</sup>H-NMR spectroscopic studies have been reported [33] on the solution conformational properties of cyclic analogues related to dermorphin in polar solvents. Previously we have described [34] investigations into the secondary structures of the polypeptide isomers used in the present study, **1** and **2**, in terms of their percentage of  $\alpha$ -helical,  $\beta$ -sheet and random coil content as determined by 2-dimensional <sup>1</sup>H-nuclear magnetic spectroscopic (2D-NMR) methods.

The present investigation introduces an alternative approach to examine the thermodynamic

behaviour and topological similarities of such polypeptides in lipophilic environments. Because they have the same composition, polypeptides **1** and **2** represent very useful probes to validate thermodynamic models for polypeptide–non-polar ligand interactions. To this end, the influence of different experimental conditions on the interactive behaviour of these polypeptides has been investigated, using a *n*-octylsilica sorbent and low pH, binary solvent–water mixtures containing either acetonitrile or methanol at different percentages. Changes in the relevant thermodynamic ( $\Delta H_{assoc,i}^o$ ,  $\Delta S_{assoc,i}^o$  and  $\Delta C_{p,i}^o$ ) and extrathermodynamic (*S*-value) parameters were then assessed as the temperature, *T*, was systematically varied. The results of this investigation with the topologically similar all L- $\alpha$ - and all D- $\alpha$ -retro-enantiomer polypeptide isomers, **1** and **2**, provide important insight into the molecular basis of these inter-linked thermodynamic and extra-thermodynamic processes that have their origin in the interaction of the polypeptides with immobilised non-polar ligates, including the influences of solvational and conformational effects that can arise at different temperatures and under different solvent conditions.

## 2. Experimental procedures

### 2.1. Apparatus

All measurements were performed on a Hewlett Packard HP1090 instrument (Hewlett Packard, Waldbronn, FRG) and a HP Chemstation with peak profiles monitored at 215 nm. Analysis of the experimental data was performed using various software packages, including the *Hephaestus* program, developed in this laboratory and compatible with the SigmaPlot version 2.0 and Excel version 5.0 software. Temperature was controlled by immersing the column in a thermostated column coolant-jacket coupled to a recirculating cooler or heater (Colora Messtechnik GmbH Lorchwutt, FRG). The various van't Hoff studies were performed with Zorbax 300SB-C8 (Rockland Technologies, Inc., USA) packed into columns with dimensions of 150  $\times$  4.6 mm i.d.

### 2.2. Chemicals and reagents

Acetonitrile (HPLC grade) was obtained from Biolab Scientific Pty Ltd (Sydney, Australia), methanol (HPLC grade) from E. Merck (Kilsyth, Australia) and trifluoroacetic acid (TFA) from Auspep Pty Ltd (Melbourne, Australia). Water was distilled and deionised in a Milli-Q system (Millipore, Bedford, MA, USA). The all L- $\alpha$ - and the retro-D- $\alpha$ -polypeptides, DDALYDDKNWDRAPQRCYYQ and QYYCRQPARDWNKDDYLADD, **1** and **2**, respectively, were synthesised by standard Fmoc solid phase peptide synthesis procedures and characterised by standard analytical procedures (ES-MS, CZE,  $^1\text{H}$ -2D-NMR, amino acid analysis) as described elsewhere [35].

### 2.3. Circular dichroism measurements

Circular dichroism (CD) spectra were performed on a J-700 spectropolarimeter (Jasco, Japan). The temperature was maintained at 293 K unless otherwise noted. Sampling of data was done every 0.2 nm using a bandwidth of 1.0 nm and a response time of 1 s. The scan speed was 10 nm/min, and each spectrum was averaged from four individual scans. CD measurements of the polypeptides **1** (387.8  $\mu\text{M}$ ) and **2** (340.7  $\mu\text{M}$ ) were performed at 190–250 nm in a 200- $\mu\text{l}$  cell with a pathlength of 0.02 cm in the following buffers: (a) 20% ACN, 0.09% TFA (pH 2.1); (b) 40% TFE (pH 2.3) at 288 K; (c) 100 mM phosphate, 50 mM SDS (pH 4.4); and (d) 300 mM SDS (pH 2.6) at 298 K. At concentrations above 500  $\mu\text{M}$  polypeptide self-association was evident. All data from the J-700 spectro-polarimeter were acquired and handed by an evaluation program J-700 (Jasco, Japan). CD spectra from the raw data spectra were obtained after performing noise reduction using fast Fourier transformation (FFT). The influence of different concentrations were taken into account, with the baseline compensated spectra (obtained after subtraction of a corresponding blank) normalised to allow comparison of the spectra of the polypeptides.

## 2.4. Amino acid analysis

Amino acid compositional analyses were carried out to determine the peptide concentrations using a Waters Picotag Amino Acid Analyser (Milford, MA, USA).

## 2.5. Van't Hoff measurements and experimental procedures

Bulk solvents were filtered and degassed by sparging with helium. Measurements were performed using 0.09% TFA with the acetonitrile or methanol contents in water within the range 17–21% v/v or 35–40% v/v, respectively, in increments of 1%, at a flow rate of 1 ml/min and at temperatures of 278, 283, 288, 293, 298, 303, 308, 313, 318, 323, 328, 333 and 338 K, respectively. Solutions of the 20-mer polypeptides, **1** and **2**, were prepared by dissolving the polypeptides at a concentration of 0.4 mg/ml in 0.09% (v/v) TFA. Injection sizes varied between 2 and 8  $\mu$ g. Under these concentration and mass loading conditions, the polypeptides **1** and **2** exist in solution as monomeric species as assessed by circular dichroism and 2D- $^1$ H-NMR measurements [34]. All data points were derived from at least duplicate measurements. The column dead volume and phase ratio of the system was determined as described elsewhere [17] with the non-interactive solute, sodium nitrate. The various thermodynamic parameters were calculated using the *Hephaestus* software developed in this laboratory, coupled to the Excel version 5.0 software program, whilst the statistical analysis involving Excel- and Sigmapstat-based linear and non-linear regression analysis. In all figures presented, the standard deviations of replicates were  $< \pm 5\%$  and typically smaller than the size of the data points.

## 3. Results and discussion

### 3.1. Theoretical background

The interaction of a polypeptide,  $P_i$ , with a non-polar ligate(s) can be described in terms of the logarithm of the capacity factor,  $\log k'_i$ , which

can be related from fundamental thermodynamic considerations to the temperature,  $T$ , through the expression:

$$\log k'_i = -\Delta H_{assoc,i}^o/RT + \Delta S_{assoc,i}^o/R + \log \Phi \quad (2)$$

where  $R$  is the gas constant,  $\Delta H_{assoc,i}^o$  and  $\Delta S_{assoc,i}^o$  are the changes in enthalpy and entropy associated with the interaction and  $\log \Phi$  is the phase ratio of the system, i.e. the logarithm of the ratio of the stationary phase volume,  $V_s$ , to the mobile phase volume,  $V_m$ , within a column for a defined chromatographic sorbent and mobile phase composition.

As noted above, for a non-polar ligate system where the phase ratio and the properties of the solute and the hydrophobic surface of the sorbent are invariant with temperature, then the values of  $\Delta H_{assoc,i}^o$  and  $\Delta S_{assoc,i}^o$  associated with the interaction of  $P_i$  with the non-polar ligates can be derived in the traditional manner by linear regression analysis of the  $\log k'_i$  vs.  $1/T$  van't Hoff plots from the slope and intercept values, respectively. In the case of a polypeptide–non-polar ligate interactions based on the use of an  $n$ -alkylsilica, the extent of fit of the experimental data to the linearised form of the van't Hoff dependency thus provides insight into whether linear (Langmuirean) adsorption/desorption conditions prevail or whether additional factors are involved in the polypeptide (or protein) interaction with the non-polar ligates, e.g. whether stabilisation/destabilisation of the secondary or tertiary structure of  $P_i$  occurs under the perturbing conditions of the interaction.

Detailed analysis of the characteristics of the  $\log k'_i$  vs.  $1/T$  dependency as a function of  $T$  thus has the potential to provide insight into whether the mechanism of the interaction of  $P_i$  with the hydrophobic surface involves the participation of secondary equilibrium processes that are dependent on temperature. As shown previously [11,18], three situations can be contemplated for the interaction of a polypeptide or protein with an hydrocarbonaceous ligate, whereby the change in heat capacity,  $\Delta C_{p,i}^o$ , of the

system (i) is zero and remains invariant with regard to temperature (the isothermic scenario); (ii) is not zero and is linearly dependent on temperature (the homothermic scenario); or (iii) is not zero and shows a (non-linear) dependency on temperature (the heterothermic scenario). In the bulk state, the heat capacity,  $C_{p,i}^o$ , of a substance is usually defined as the quantity of heat necessary to raise the temperature of a unit mass of the substance by 1 K. Analogous expressions can be applied to a ligate–ligand system, such as a polypeptide interacting with immobilised *n*-alkyl chains, provided the characteristics of state of a unit cell of the solvated polypeptide–ligate complex can be defined. Under these conditions, when a unit mass of the ligand–ligate–solvent system initially in a state defined by  $P$ ,  $V$  and  $T$  undergoes a small change defined by  $\delta P$ ,  $\delta V$  and  $\delta T$ , then a change in a particular parameter or quantity,  $U$ , associated with the ligate–ligand interaction may be represented by the equations of state as a function of  $P$ ,  $V$  and  $T$  such that

$$\Delta U = \frac{\partial U}{\partial P} \Delta P + \frac{\partial U}{\partial V} \Delta V + \frac{\partial U}{\partial T} \Delta T \quad (3)$$

where  $P$  is the pressure (in Pascal units),  $V$  is the molar volume and  $T$  is the absolute temperature in degrees Kelvin.

Accordingly, the change in the internal energy,  $\Delta E$ , of the system can be written in terms of the change in entropy,  $\Delta S_{assoc,i}^o$ , by the perfect differential

$$dE = TdS - PdV \quad (4)$$

where

$$\left( \frac{\partial E}{\partial S} \right)_V = T, \quad \left( \frac{\partial E}{\partial V} \right)_S = -P$$

and

$$\left( \frac{\partial T}{\partial V} \right)_S = - \left( \frac{\partial P}{\partial S} \right)_V \quad (5)$$

Similarly, the change in enthalpy of association,  $\Delta H_{assoc,i}^o$ , of the system can be defined in terms of the internal energy,  $E$ , such that

$$H = E + PV \quad (6)$$

or

$$dH = TdS + VdP \quad (7)$$

and hence

$$\left( \frac{\partial T}{\partial P} \right)_S = \left( \frac{\partial V}{\partial S} \right)_P \quad (8)$$

The change in heat capacity,  $\Delta C_{p,i}^o$ , for a polypeptide–non-polar ligate system as a function of  $T$  can be expressed according to the Kirchoff relationships [36,37] as:

$$\Delta C_{p,i}^o = T \partial S_{p,i}^o / \partial T \quad (9)$$

where

$$\Delta S_{assoc,i}^o = \int \frac{\Delta C_{p,i}^o}{T} dT \quad (10)$$

and

$$\Delta C_{p,i}^o = \partial H_{assoc,i}^o / \partial T \quad (11)$$

where

$$\Delta H_{assoc,i}^o = \int \Delta C_{p,i}^o dT \quad (12)$$

and

$$\Delta C_{p,i}^o \partial T = \partial E + P \partial V - \mu_i \partial \mu_i \quad (13)$$

where  $\partial E$  represents the incremental difference in the internal energy of the system. According to Eq. (13),  $\Delta C_{p,i}^o$  is also related to the change in the standard enthalpy and the standard pressure–volume product ( $\partial PV$ ) terms, whilst the term  $\mu_i$  takes into account contributions from processes not defined by the criteria of the Stefan–Boltzmann–Maxwell law. If the interaction of  $P_i$  with the immobilised ligates satisfies these criteria, i.e. no effects other than standard changes in  $P$ ,  $V$  and  $T$  are involved, then Eq. (7) becomes

$$\Delta C_{p,i}^o \partial T = \partial E + P \partial V \quad (14)$$

and hence

$$\Delta C_{p,i}^o \partial T = \partial H_{assoc,i}^o - \partial(PV) + P\partial V \quad (15)$$

or

$$\Delta C_{p,i}^o \partial T = \partial H_{assoc,i}^o - V\partial P \quad (16)$$

Evaluations of the interaction of  $P_i$  with the hydrocarbonaceous ligates in terms of Eqs. (6)–(16), however, do not represent complete descriptions of the binding process, because the condition(s) under which the thermal energy of the system is increased has not been specified. If the heat capacity of the system is increased under experimental conditions where the pressure,  $P$ , does not change significantly, then Eq. (16) can be simplified and the specific heat capacity can be defined in terms of Eq. (17) as follows:

$$C_{p,i}^o \partial T = (\partial H_{assoc,i}^o)_P \quad (17)$$

or

$$C_{p,i}^o = (\partial H_{assoc,i}^o / \partial T)_P \quad (18)$$

In RP-HPLC, when the temperature of the system is changed, the viscosity,  $\eta$ , of an aquo-organic solvent mobile phase will also change. This variation in viscosity will result in change in pressure ( $\Delta P$ ) according to the relationship

$$\Delta P = \frac{\eta \eta L}{\varepsilon_p d_p^2} \quad (19)$$

where  $u$  is the linear flow velocity of the eluent,  $L$  is the length of the column,  $\varepsilon_p$  is the specific permeability of the sorbent, and  $d_p$  is the average particle diameter. Over the temperature range employed in the present investigations, the  $\Delta P$  variations for the well-packed columns usually did not exceed approximately 15% of the original pressure drop, i.e. from 240 bar at 10°C to 210 bar at 50°C for the water-based eluents, for the modern pressure-damped instrumentation used with the standard HPLC columns of dimensions 150 × 4.6 mm i.d. containing the spherical  $n$ -alkylsilica sorbent of average particle diameter of 6  $\mu\text{m}$ .

Although constant pressure conditions can be achieved by adjusting the linear flow velocity of the eluent by a corresponding percentage, in practice this approach experimentally requires special flow constriction or stream splitting equipment, which is usually unavailable to most investigators. A further factor must also be considered when the linear flow velocity is adjusted. Because of the dependency of the column void time,  $t_o$ , on  $u$ , i.e.  $t_o = (L \times F)/u$ , where  $L$  is the column length and  $F$  is the flow rate, changes in  $u$  will, most importantly, affect directly the  $k'_i$  value of a polypeptide,  $P_i$ , eluted under isocratic conditions, since  $k'_i = (t_{p,i} - t_o)/t_o$ . Isocratic conditions at constant flow rate should thus be employed for the measurement of thermodynamic parameters associated with the interaction of polypeptides with the non-polar ligates in RP-HPLC systems. When RP-HPLC systems are operated at a constant flow rate, the effect of operating at an average back pressure of  $\approx 225$ , 250 or alternatively 275 bar on the  $k'_i$  of solutes has been found to be small, as evident from the essentially constant  $k'_i$  values found for non-polar or neutral compounds [38]. Even when extremely high pressure changes exceeding 2 kbar are generated from an initial value of  $\approx 4$  kbar with specialised RP-HPLC systems, e.g. micro-bore columns with inner diameter of 30  $\mu\text{m}$  packed with 1.5- $\mu\text{m}$  non-porous  $n$ -alkylsilica particles, variations in the  $k'_i$  values of moderately retained solutes are still relatively small (i.e.  $\Delta k'_i < 2$ ) [39]. Such large pressure variations are outside the operational range examined in most laboratory investigations and were not achieved during any of the present series of experiments. Moreover, at pressures of  $\approx 200$  bar, the partial molar volumes,  $V$ , of polypeptides are expected to remain essentially constant under these conditions. Based on these considerations, the effect of the product terms, namely  $V\partial P$  and  $P\partial V$  [e.g. Eq. (16)], on the thermodynamic parameters  $\Delta H_{assoc,i}^o$ ,  $\Delta S_{assoc,i}^o$  or  $\Delta C_{p,i}^o$  will be small or tend to zero. Application of Eqs. (7)–(18) thus provides a useful and appropriate approximation of the ligand–ligate interaction, enabling evaluation of the relationship between  $k'_i$ ,  $T$  and the associated thermodynamic parameters  $\Delta H_{assoc,i}^o$ ,  $\Delta S_{assoc,i}^o$  and  $\Delta C_{p,i}^o$  for a

defined polypeptide solute, flow rate and mobile phase composition with immobilised lipophilic ligands.

The equilibrium association constant,  $K_{assoc,i}$ , for the interaction of  $P_i$  with the hydrophobic surface is a function of temperature, with the dependency taking the form:

$$K_{assoc,i} = e^{-\Delta G_{assoc,i}/RT} \quad (20)$$

where the value of the Gibbs free energy change for the interaction,  $\Delta G_{assoc,i}^o$  is a function of temperature only. By substituting and re-arranging the relevant terms of Eq. (20), the following dependencies are as a consequence derived:

$$\partial \log K_{assoc,i} = -1/R \times [(T \times \partial G_{assoc,i}^o)/T^2] \quad (21)$$

From Eq. (1), Eq. (21) can be arranged such that

$$\partial \log K_{assoc,i}/\partial T = \Delta H_{assoc,i}^o/RT^2 \quad (22)$$

Moreover, the equilibrium association constant,  $K_{assoc,i}$ , for the binding of the polypeptide to the ligate related to the capacity factor,  $k'_i$ , through the relationship:

$$\log K_{assoc,i} = \log k'_i + \log \Phi \quad (23)$$

and hence

$$\partial \log k'_i/\partial T = \Delta H_{assoc,i}^o/RT^2 \quad (24)$$

In situations whereby  $\Delta H_{assoc,i}^o$  and  $\Delta S_{assoc,i}^o$  are both invariant with temperature, i.e. under isothermic binding conditions whereby over a range of temperatures linear van't Hoff plots are observed, then the following expression is obtained:

$$\log k'_i = -\Delta H_{assoc,i}^o/RT + I \quad (25)$$

with the term  $I$  incorporating contributions from both the entropic and the phase ratio terms in the form  $I = \Delta S_{assoc,i}^o/R + \log \Phi$ . If the phase ratio is assumed (or found) to be independent of temperature, then the plots of  $\log k'_i$  vs.  $1/T$  will gener-

ate a straight line characteristic of linear van't Hoff plots. Thermodynamic data for a large number of low molecular weight solutes have been measured by chromatographic procedures, interpreted in terms of this linear van't Hoff relationship [Eq. (25)] and the integrity of the derived data firmly established [40–43] from independent measurements, such as partition coefficient with octanol–water systems or aqueous solubility determinations.

Several different experimental approaches can be employed to assess the extent of change of the phase ratio of a chromatographic system with temperature or another experimental condition. Although classical volumetric or gravimetric methods have proved unsuitable to measure the values of the stationary phase volume,  $V_s$ , or mobile phase volume,  $V_m$ , and thus the phase ratio ( $\Phi = V_s/V_m$ ), the tracer pulse method [44] with isotype probe solutes represents a convenient experimental procedure to determine  $V_s$  and  $V_o$ , where  $V_o$  is the thermodynamic dead volume of the column packed with a defined chromatographic sorbent [45]. The value of  $V_m$  can be then calculated from the expression  $V_m = V_o - V_s$ . In addition, the true value of  $V_m$  can be independently measured using an analyte that is not adsorbed to the sorbent and resides exclusively in the mobile phase. Sodium nitrate, as employed in this investigation, has been previously found appropriate [14,17,18] for such measurements with *n*-alkylsilica sorbents. As a further independent measure, the extent of change of  $\Phi$  with  $T$  can be assessed with weakly interacting neutral or non-polar solutes that show linear dependencies of  $\log k'_i$  vs.  $1/T$  over a large  $T$  range at a defined mobile phase composition [3,15]. Experimental data derived as part of our investigations demonstrated that  $\Phi$  changes at a specified solvent composition were relatively small, i.e.  $\Delta\Phi \leq \pm 10\%$  over the examined  $T$  range for the *n*-octylsilica reversed phase system used and hence the contribution from the  $\log \Phi$  term to the  $k'_i$  changes [Eqs. (2) and (23)] will be small and essentially constant. On the other hand, if the corresponding  $K_{assoc,i}$  value remains constant for a specified polypeptide,  $P_i$ , in order to achieve a significant changes in  $k'_i$ , such as the



$\geq 20$ -fold variations observed with polypeptide **1** and **2** in this study then, according to Eq. (23), a change in  $\Phi$  of  $\geq 20$ -fold would also have to occur. For such  $\Phi$  changes to arise, a simple experimental expediency must be invoked, whereby the surface area-to-volume ratio of the stationary phase support material is changed by a corresponding amount. This effect can only be achieved [41] by utilising non-porous spherical silica particles with a surface coating of the same polarity and same nominal mean particle diameter but with surface areas in the range of 0.02–1 m<sup>2</sup>/g instead of the commonly used, highly porous *n*-alkyl-modified silica particles with surface areas of 5–350 m<sup>2</sup>/g. In the present investigation, the same chemically-modified reversed phase sorbent was thus used throughout to ensure that any contribution to the interactive behaviour of the polypeptides, **1** and **2**, from the effects of  $T$  on  $\Phi$  was maintained at a small or negligible value compared to the dependencies of  $K_{assoc,i}$ , and hence  $\Delta H_{assoc,i}^o$  or  $\Delta S_{assoc,i}^o$ , on  $T$ .

When  $\Delta H_{assoc,i}^o$  and  $\Delta S_{assoc,i}^o$  are dependent on temperature, then plots of  $\log k'_i$  vs.  $1/T$  will not follow linear dependencies. According to Kirchhoff's law, when temperature-dependent heat capacity conditions prevail, i.e. when  $\Delta C_{p,i}^o \neq 0$  as anticipated for the temperature-dependent homothermic and heterothermic scenarios, respectively, then the dependency of  $\log k'_i$  on  $T$  can be approximated by a polynomial expression as represented by Eq. (26):

$$\log k'_i = a + b(1/T) + c(1/T)^2 + d(1/T)^3 + \dots + \ln \Phi \quad (26)$$

and thus

$$\partial \log k'_i / \partial T = [\partial \log k'_i / \partial (1/T)] \times [\partial (1/T) / \partial T] \quad (27)$$

$$= -(1/T)^2 \times \left[ b + 2c(1/T) + 3d(1/T)^2 + \dots \right] \quad (28)$$

In these homothermic and the heterothermic sce-

narios, the change in enthalpy can be thus represented by

$$\Delta H_{assoc,i}^o = -R \times \left[ b + 2c(1/T) + 3d(1/T)^2 + \dots \right] \quad (29)$$

whilst the change in heat capacity can be represented as

$$\Delta C_{p,i}^o = \partial \Delta H_{assoc,i}^o / \partial T \quad (30)$$

$$= m/(T)^2 + n/(T)^3 + \dots \quad (31)$$

where  $m = 2Rc$  and  $n = 6Rd$ , etc.

When non-linear plots of  $\log k'_i$  vs.  $1/T$  are observed, under some circumstances  $\Delta H_{assoc,i}^o \rightarrow 0$  and  $\log k'_i$  may thus reach a maximal value at a temperature corresponding to  $T_H$  since the slope of the plots of  $\log k'_i$  vs.  $1/T$  at any temperature will proportional to the  $\Delta H_{assoc,i}^o$  value at that temperature [46]. In these circumstances, when  $\log k'_i$  reaches a maximal value as  $T$  is varied and  $\Delta C_{p,i}^o$  is constant for the process, the dependency of the  $\Delta H_{assoc,i}^o$  and  $\Delta S_{assoc,i}^o$  contributions on temperature can be expressed in terms of  $\Delta C_{p,i}^o$  as:

$$\Delta H_{assoc,i}^o = \Delta H_{assoc,i}^* + \Delta C_{p,i}^o (T - T_H^*) \quad (32)$$

and

$$\Delta S_{assoc,i}^o = \Delta S_{assoc,i}^* + \Delta C_{p,i}^o \log (T/T_S^*) \quad (33)$$

where the symbols  $T_H^*$  and  $T_S^*$  refer to the isenthalpic and isentropic temperatures at which the plots of  $\Delta H_{assoc,i}^o$  vs.  $T$  or  $\Delta S_{assoc,i}^o$  vs.  $T$ , respectively, for the polypeptides (or proteins) intercept and attain a common value of  $\Delta H_{assoc,i}^*$  or  $\Delta S_{assoc,i}^*$ , respectively, under the different experimental conditions. When such ligand–ligate processes prevail, then the dependency of  $\log k'_i$  on  $T$  can also be approximated by the logarithmic expression [47]:

$$\log k'_i = \frac{\Delta C_{p,i}^o}{R} \left( \frac{T_H}{T} - \log \frac{T_S}{T} - 1 \right) + \log \Phi \quad (34)$$

From Eqs. (26)–(34), values of  $\Delta H_{assoc,i}^o$ ,  $\Delta S_{assoc,i}^o$  or  $\Delta C_{p,i}^o$  corresponding to homothermic and heterothermic interaction processes for polypeptides, **1** and **2** (or any other polypeptide or protein) can, thus, be evaluated from the non-linear van't Hoff plots using methods based on non-linear least squares regression and associated curve fitting procedures.

### 3.2. Thermodynamic and extra-thermodynamic features of the interaction of polypeptide **1** and **2** with the lipophilic *n*-octyl ligate groups

In order to thus further characterise in terms of the above thermodynamic relationships polypeptide–hydrophobic ligate interactions in the presence of aquo-acetonitrile or aquo-methanol mixtures, the binding data for the polypeptide pair, L- $\alpha$ -DDALYDDKNWDRAPQRCYYQ, **1**, and its retro-all D- $\alpha$ -QYYCROPARDWNKDDYLADD, **2**, isomer were determined with a *n*-alkylsilica as a function of *T* and organic solvent volume fraction,  $\varphi$ . These two polypeptides are composed of the same amino acid residues but because polypeptide **2** involves a reversal of the direction of the amino acid sequence, and an inversion of the chirality at the  $\alpha$ -carbon atom of the side chain of each residue, the peptide backbone of polypeptide **2** can, in principle, assume the same topological shape in solution as polypeptide **1**. The similarity of the solution conformations of these two polypeptides has been documented in our earlier investigations [34,35] based on high field  $^1\text{H}$ -2D-nuclear magnetic resonance procedures. Shown in Fig. 1 are the circular dichroism (CD) spectra of the polypeptides **1** and **2** in the presence of the following  $\alpha$ -helix inducing buffers (a) 20% ACN, 0.09% TFA (pH 2.1); (b) 40% TFE (pH 2.3) at 288 K; (c) 100 mM phosphate, 50 mM SDS (pH 4.4); or (d) 300 mM SDS (pH 2.6) at 298 K. As expected for compound pairs involving inversion of chirality at each  $\alpha$ -carbon atom, these polypeptides exhibit mirror image CD spectra in solution with partial induction of some  $\alpha$ -helical content under the experimental conditions used.

The plots of  $\log k'_i$  vs. the volume fraction,  $\varphi$ , of the organic solvent, acetonitrile and methanol, for the L- $\alpha$ -polypeptide, **1**, and its retro-inverso

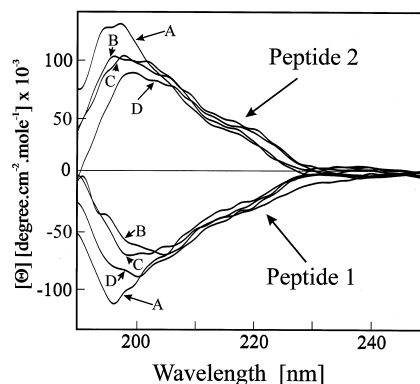


Fig. 1. CD spectra of the polypeptides, **1** and **2**, measured under different solvent conditions: (a) 20% ACN, 0.09% TFA (pH 2.1) at 288 K; (b) 40% TFE (pH 2.3) at 288 K; (c) 100 mM phosphate, 50 mM SDS (pH 4.4) at 298 K; or (d) 300 mM SDS (pH 2.6) at 298 K. Other conditions are described in Section 2.

isomer, **2**, determined over the range of  $\varphi = 0.17$  to  $\varphi = 0.21$  with the water–acetonitrile mixtures and from  $\varphi = 0.35$  to  $\varphi = 0.40$  with the water–methanol mixtures, respectively, and from temperatures of 278 K to 338 K in 5-K increments are shown in Fig. 2a–d, respectively. As evident from these data, the change in  $\log k'_i$  values was  $\geq 2.5$  over this temperature range for most of the mobile phase conditions. For these polypeptides, the trend that was expected for the hydrophobic effect dominating the interaction mechanism was observed, with  $\log k'_i$  decreasing values as the  $\varphi$ -value was increased. In Fig. 3a–d are shown the corresponding three-dimensional grid plots for the *S*-values of these two polypeptides as the temperature and  $\varphi$ -values were systematically varied. As documented elsewhere [11,19], the *S*-value of a polypeptide in the presence of a reversed phase sorbent can be related to extra-thermodynamic parameters, such as the accessible molecular surface area,  $\Delta A_{mol}$ , through the expression

$$S = a'\Delta A_{hyd} + b'\kappa^e + c' \quad (35)$$

where  $\Delta A_{hyd}$  is the hydrophobic contact area (proportional to the accessible molecular surface area,  $\Delta A_{mol}$ ),  $\kappa^e$  is a solvophobic cavity factor

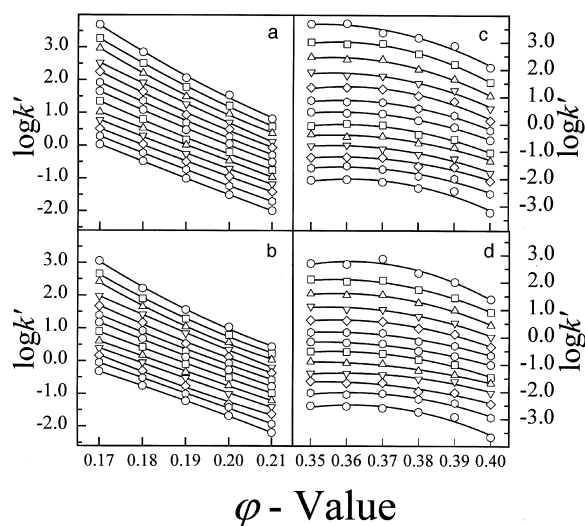


Fig. 2. Plot of  $\log k'_i$  vs. the volume fraction,  $\phi$ , for the polypeptides, **1** and **2**, with the acetonitrile– (a,b) and methanol– (c,d) water mixtures at different temperatures. In each panel the data shown as the top  $\log k'_i$  vs.  $\phi$  plot (shown as the  $\bullet$ – $\bullet$  values) corresponds to  $T = 278$  K and the bottom  $\log k'_i$  vs.  $\phi$  plot (shown as  $\bullet$ – $\bullet$  values) corresponds to  $T = 338$  K, respectively.

related to the ratio in energy required for the formation of a cavity with surface area equal to  $\Delta A_{mol}$  and the energy required to extend the planar surface of the liquid by the same area, and  $a'$ ,  $b'$  and  $c'$  are constants related to the molecular properties of the polypeptide. In each case, the  $S$ -values for **1** and **2** were derived by regression analysis methods from the gradient of the experimental plots of  $\log k'_i$  vs.  $\phi$  at specified  $\phi$  and  $T$  values with the regression coefficients typically  $\geq 0.9985$ .

The overall similarity of the  $\log k'_i$  vs.  $\phi$  data sets for **1** and **2** with acetonitrile or alternatively with methanol (cf. Fig. 2a with Fig. 2b; or Fig. 2c with Fig. 2d) and their derived 3-D plots (cf. Fig. 3a with Fig. 3b; or Fig. 3c with Fig. 3d) confirms that these two 20-mer polypeptides exhibit similar interactive behaviour, and thus can assume similar conformational properties, when in the same hydrophobic environment. However, it can be noted from the comparison of the acetonitrile vs. the methanol solvent systems shown in Fig. 2a–d, and particularly from comparison of the data shown in Fig. 3a–d, that depending on the choice

of solvent composition significant changes in the shapes of these plots arise at a specific temperature for these polypeptides. As evident from the data shown in Fig. 2a,b and Fig. 3a,b; with the water–acetonitrile mixtures (as well as with the water–methanol mixtures shown in Fig. 2c,d and Fig. 3c,d) small but nevertheless significant differences are also evident between the interactive behaviour of **1** and **2** under some conditions of temperature and solvent mole fraction. In associated studies [11], we have observed analogous differences in the local conformations of specific amino acid residues in the NOESY 2D- $^1\text{H}$ -NMR spectra of these polypeptides acquired under different solvent conditions at 500 MHz and 600 MHz in 40% deuterio-trifluoroethanol ( $d_3$ -TFE)/ $\text{H}_2\text{O}$  at pH 2.3, or in 300 mM sodium dodecylsulphate in 100%  $\text{D}_2\text{O}$  or 90%  $\text{H}_2\text{O}/10\%$   $\text{D}_2\text{O}$  at pH 2.6, although overall the conformations of both polypeptides were very similar. In particular, the predominant conformation observed for **1** and **2** under these solution conditions incorporates a central  $\alpha$ -helical region which extends over the same series of amino acid residues in each peptide;  $\text{Y}^5\text{DDKNWDRA}^{13}$  in polypeptide **1** and  $\text{A}^8\text{RDWNKDDY}^{16}$  in polypeptide **2**. The C- and N-terminus of each peptide have an extended, random coil structures in solution. The results from this earlier study and the present investigation highlight the influence that the D- $\alpha$ -Pro residue in the polypeptide **2** (at position 7) can have in terms of subtle  $\beta$ -turn constraint differences around this residue compared to the L- $\alpha$ -Pro residue in the corresponding all L- $\alpha$ -polypeptide **2** (at the inverso-image sequence position 14). These investigations thus collectively provide the first definitive indication that the conformations of retro-inverso-polypeptides and their all L- $\alpha$ -amino acid isomers can assume similar topologies in the presence of aquo-organic solvent mixtures and lipophilic solid–liquid interfaces. These findings are also relevant to the conformational features that these polypeptides can assume in the presence of lipid bilayers.

The plots of vs.  $1/T$  for the L- $\alpha$ - and retro-all D- $\alpha$ -polypeptides, **1** and **2**, determined at different  $\phi$ -values with water–acetonitrile and water–methanol mixtures containing 0.09% TFA are

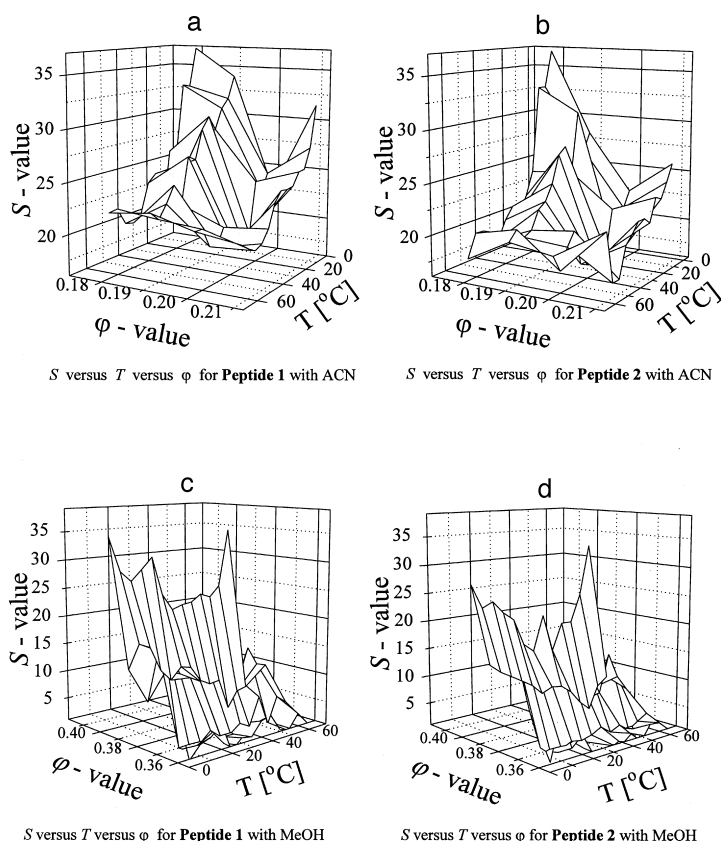


Fig. 3. 3D grid plots of  $S$  vs.  $\phi$  vs.  $T$  for the polypeptides, **1** and **2**, for the acetonitrile– (a,b) and the methanol– (c,d) water systems.

shown in Fig. 4a–d. In all cases higher values of the correlation coefficients ( $r^2 \geq 0.9960$ ) were obtained when the experimental data for this polypeptide pair were fitted to the second order quadratic expression corresponding to the  $\log k'_i$  vs.  $1/T$  dependency [e.g. Eq. (26), where  $d, e, \dots = 0$ ] rather than a first order dependency related to the van't Hoff relationship. This trend in the  $\log k'_i$  vs.  $1/T$  data, involving non-linear dependencies of the van't Hoff plots, has been noted previously as part of our investigations [19,20] into the interactive behaviour of the hormonal polypeptides  $\beta$ -endorphin, glucagon and bovine insulin at different temperatures with immobilised *n*-butyl and *n*-octadecyl groups.

The characteristic shapes for the plots of  $\log k'_i$  vs.  $1/T$  for **1** and **2** can be interpreted in terms of the extended mean value theory that forms the

basis of Kirchoff's law. As a consequence, the values of the coefficients  $a, b, c, \dots$  of the polynomial dependency of  $\log k'_i$  vs.  $1/T$  can be readily derived by regression analysis utilising the *Hephaestus* software based on Eqs. (26)–(34). Concomitantly, it is possible to calculate the corresponding  $\Delta H_{assoc,i}^o$ ,  $\Delta S_{assoc,i}^o$  and  $\Delta C_{p,i}^o$  values from these non-linear plots of  $\log k'_i$  vs.  $1/T$  at different solvent compositions. Since in the case of the polypeptides **1** and **2**, the  $\log k'_i$  values increased with decreasing  $T$ , but did not reach maximum values over the examined range of  $T$  values, plots of  $\Delta H_{assoc,i}^o$  vs.  $T$ ,  $\Delta S_{assoc,i}^o$  vs.  $T$  and  $\Delta C_{p,i}^o$  vs.  $T$  were generated for polypeptides **1** and **2** utilising the *Hephaestus* software subroutines with the experimental data fitted to Eqs. (26)–(29). However, in other studies ([18]; Boysen and Hearn, unpublished results) we have found with

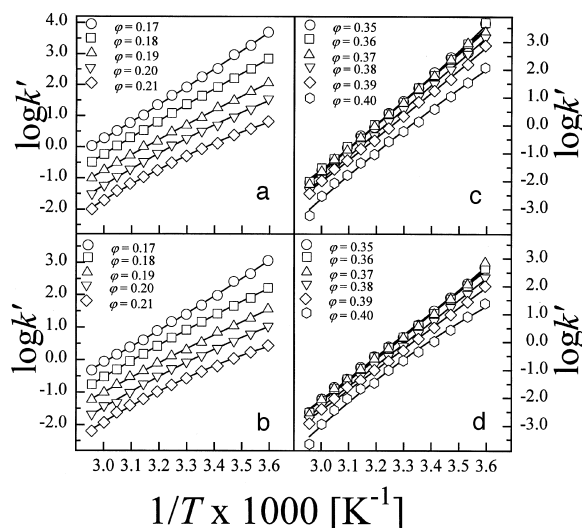


Fig. 4. Plots of  $\log k'_i$  vs.  $1/T$  for polypeptides, **1** and **2**, for the acetonitrile– (a,b) and the methanol– (c,d) water systems at different  $\varphi$ -values.

larger polypeptides and small globular proteins, such as insulin, the transcription factors *fos* and *jun* or cytochrome *c* variants, the corresponding plots of  $\log k'_i$  vs.  $1/T$ , as well as the derived  $\Delta H_{assoc,i}^o$  vs.  $T$  and  $\Delta S_{assoc,i}^o$  vs.  $T$  plots, reach maximum values at different  $\varphi$ -values.

As shown in Fig. 5 (for the acetonitrile system) and Fig. 6 (for the methanol system) essentially linear dependencies were observed between  $\Delta H_{assoc,i}^o$ ,  $\Delta S_{assoc,i}^o$  or  $\Delta C_{p,i}^o$  and  $T$ . Since in all cases  $\Delta C_{p,i}^o$  was not constant, with  $\Delta C_{p,i}^o \neq 0$ , these results are consistent with heterothermic processes occurring for the interaction of these 20-mer polypeptides with the *n*-octylsilica sorbent in the different aquo-acetonitrile and aquo-methanol solvent environments. It is interesting to note that although the  $\Delta H_{assoc,i}^o$  and  $\Delta S_{assoc,i}^o$  values were negative, the slopes of these  $\Delta H_{assoc,i}^o$  vs.  $T$  and  $\Delta S_{assoc,i}^o$  vs.  $T$  plots were dependent on the volume fraction,  $\varphi$ , of the solvent composition, resulting in these plots intersecting at convergent values near to  $T = 320$ – $330$  K. Similarly, the slopes of the  $\Delta C_{p,i}^o$  vs.  $T$  plots for both the acetonitrile and the methanol systems were also essentially linear, reaching (hypothetically) a convergent common value of  $\Delta C_{p,i}^o$  at an extrapolated value of  $T$  of approximately  $T_{\Delta C_p} = 450$  K. Acetonitrile is known to be a poor hydrogen bond

acceptor as a solvent resulting in the generation of solvent clusters with water–acetonitrile mixtures, whilst in contrast, methanol is a good hydrogen bond acceptor [48–50]. These solvent differences give rise to significant changes in the hydrogen bonding characteristics and solvation state of both the polypeptides and the immobilised *n*-alkyl chains and thus substantial differences in the overall behaviour with polypeptides in reversed phase systems. As evident from the data shown in Figs. 5 and 6, these differences in solvation properties were reflected as different slopes in the plots of  $\Delta H_{assoc,i}^o$ ,  $\Delta S_{assoc,i}^o$  or  $\Delta C_{p,i}^o$  vs.  $T$ . Moreover, because of the molecular organisation of acetonitrile, the properties of the derived binary water–solvent will, moreover, be less constraining at higher temperatures than for the hydrogen-bonding methanol-based mixtures. This behaviour was reflected in terms of both the magnitudes of the  $\Delta H_{assoc,i}^o$ ,  $\Delta S_{assoc,i}^o$  or  $\Delta C_{p,i}^o$  values per se as well as the magnitude of the changes in  $\Delta H_{assoc,i}^o$ ,  $\Delta S_{assoc,i}^o$  or  $\Delta C_{p,i}^o$  as  $T$  was systematically varied with these polypeptides.

From the above results, the conclusion can be reached that predictions based on Eqs. (26)–(33) correlate well with the experimental data for **1** and **2** under the selected experimental conditions. However, the accuracy of the heat capacity values

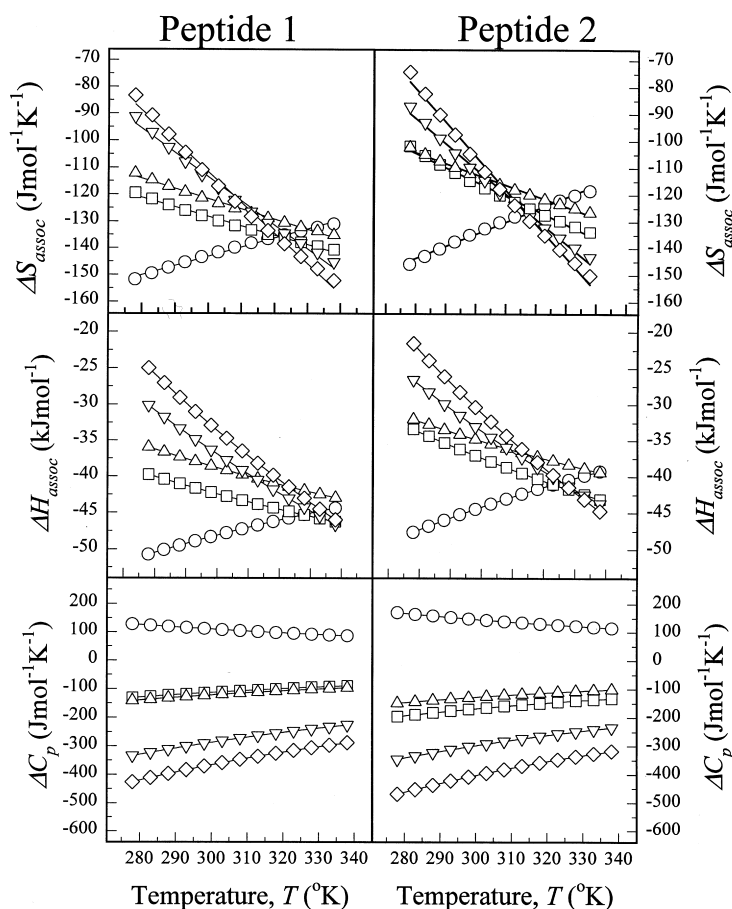


Fig. 5. Plots of  $\Delta H_{assoc,i}^o$ ,  $\Delta S_{assoc,i}^o$  and  $\Delta C_{p,i}^o$  vs.  $T$  for the polypeptides, **1** and **2**, with the acetonitrile water mixtures at different  $\varphi$ -values. The code for the  $\varphi$ -values used in the generation of these data is shown in Fig. 4.

derived from the approaches explicit to Eqs. (26)–(33) will require additional validation by calorimetric measurements with the same polypeptide-sorbent combinations before the full quantitative relevance of these chromatographically-derived values can be assessed. Precise heat capacity measurements with such heterogeneous solid-liquid systems are currently very complicated, if not impossible, to achieve with the current generation of micro-calorimetric equipment and methods of data analysis. Significant refinement in micro-calorimetric instrumentation and experimental procedures will thus be needed prior to the realisation and rigorous confirmation of the significance of  $\Delta C_{p,i}^o$  values derived by the

present approaches. The experimental data from the present investigation clearly indicate that both the changes in enthalpy and entropy of interaction for **1** and **2** with the non-polar sorbent under the different solvent conditions have strong temperature and mole fraction dependencies. For example, at low mole fraction values, the magnitude of the changes in both the enthalpy and entropy are positive as the temperature is increased, decrease with increasing mole fraction values and become at higher mole fraction values negative. Several dansyl amino acids have also been found [47] to exhibit a similar pattern of enthalpy-entropy dependencies, but to our knowledge no investigation has been previously

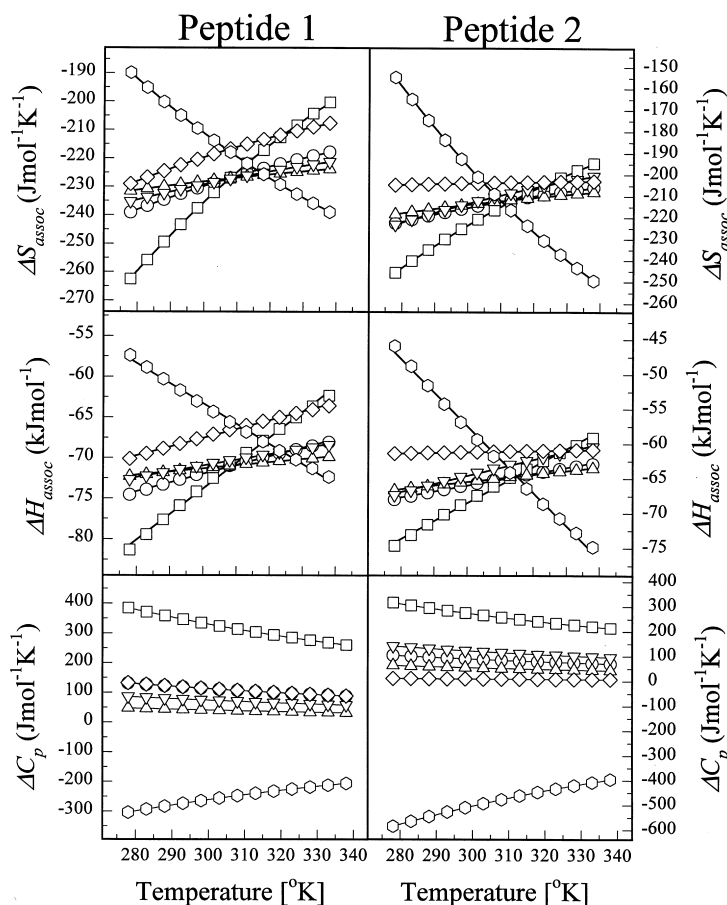


Fig. 6. Plots of  $\Delta H_{assoc,i}^o$ ,  $\Delta S_{assoc,i}^o$  and  $\Delta C_{p,i}^o$  vs.  $T$  for the polypeptides, **1** and **2**, with the methanol water mixtures at different  $\varphi$ -values. The code for the  $\varphi$ -values used in the generation of these data is shown in Fig. 4.

reported which describes similar phenomena with polypeptides or proteins in lipophilic environments.

The consequences of the type of thermodynamic behaviour manifested by the polypeptides, **1** and **2**, are clearly important, since such manifestations underpin the so-called enthalpy–entropy compensation effect observed for protein folding in bulk solution [36,51–57]. Enthalpy–entropy compensation represents a further extra-thermodynamic relationship whereby a linear dependence of  $\Delta H_{assoc,i}^o$  on  $\Delta S_{assoc,i}^o$  is predicted following a change in an experimental variable. When molecular associations between polypeptide–non-polar ligate systems involve enthalpy–entropy compensation, then large en-

thalpy changes will be associated with stronger binding and a more restricted conformation for the polypeptide in the bound state, i.e. a higher order will be induced with a concomitantly greater changes in entropy. Shown in Fig. 7a–d are the plots of  $\Delta H_{assoc,i}^o$  vs.  $\Delta S_{assoc,i}^o$  for **1** and **2** for the different solvent systems ranging from  $\varphi = 0.17$  to  $\varphi = 0.21$  with the water–acetonitrile mixtures and from  $\varphi = 0.35$  to  $\varphi = 0.40$  with the water–methanol mixtures, respectively. The linear relationship of these plots confirm that the thermodynamic behaviour of these two 20-mer polypeptides satisfies the criteria of entropy–enthalpy compensation. Moreover, the slopes of the plots with the acetonitrile-based (as well as the methanol-based) systems represent the compen-

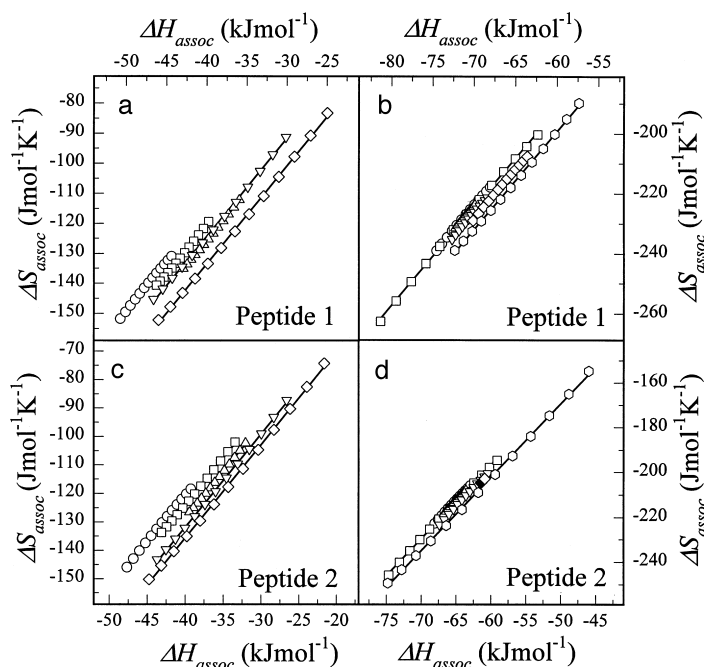


Fig. 7. Plots of  $\Delta H_{assoc,i}^{\circ}$  vs.  $\Delta S_{assoc,i}^{\circ}$  for the polypeptides, 1 and 2, with the acetonitrile– (a,b) and the methanol– (c,d) water mixtures at different  $\varphi$ -values. The code for the  $\varphi$ -values used in the generation of these data is shown in Fig. 4.

sation temperatures,  $T_{comp}$ , a characteristic parameter of the system. Since the  $T_{comp}$  values for the acetonitrile-based (as well as the methanol-based) systems at different  $\varphi$ -values were very similar, the interactions of these polypeptides with the *n*-octyl ligates at different  $\varphi$  and  $T$  values can thus be considered to be isoequilibrium processes driven by the hydrophobic effect. These observations have an important bearing on the interpretation of the molecular processes associated with surface-induced conformational changes of polypeptides and proteins in the presence of the perturbing environment of a lipophilic ligate and water–organic solvent mixtures. Such processes have been experimentally observed, but previously have only been empirically enunciated [3] in terms of the linearised form of the  $\log k'_i$  vs.  $\varphi$  dependency or in terms of a proposed linear relationship between the change in the  $S$ -value and the conformational status of the polypeptide at different  $T$  values. Importantly, the approach described in this paper provides both a theoretical as well as an experi-

mental framework to more rigorously explore the retention behaviour of polypeptides and proteins in lipophilic systems in terms of the thermodynamic and extra-thermodynamic characteristics associated with the interaction, including the influence of their molecular properties and conformational effects. Different aspects of investigations which address these latter considerations will be reported elsewhere [11,17,18].

#### 4. List of symbols and abbreviations

$a, b, c, \dots$	Coefficients for the polynomial dependency of on $\log k'_i$ $1/T$ and related to the molecular properties of the polypeptide
$a', b', c'$	Constants related to the molecular properties of the polypeptide
$c_i$	Mole fraction of the displacing solvent
$C_{p,i}^{\circ}$	Heat capacity
CD	Circular dichroism



$d_p$	Average particle diameter			quired for the formation of a cavity with surface area equal to $\Delta A_{mol}$ and the energy required to extend the planar surface of the liquid by the same area
$\Delta A_{mol}$	Accessible molecular surface area			
$\Delta A_{hyd}$	Hydrophobic contact area			
$\Delta C_{p,i}^o$	Change in heat capacity for the association of the polypeptide $P_i$ with the non-polar ligates	$k'_i$		Capacity factor $k'_i = (t_e - t_o)/t_o$
$\Delta G_{assoc,i}^o$	Change in Gibbs free energy due to the association of the polypeptide $P_i$ with the non-polar ligates	$L$		Column length
		$\log k_{o,i}$		Value of $\log k'_i$ when $c_i \rightarrow 0$ or $\varphi_i \rightarrow 0$
$\Delta H_{assoc,i}^o$	Change in the enthalpy due to the association of the polypeptide $P_i$ with the non-polar ligates	$\log k'_i$		Logarithm of the capacity factor, $k'_i$
		$\mu_i$		Non-ideal Stefan–Boltzman–Maxwell contributions
$\Delta S_{assoc,i}^o$	Change in the entropy due to the association of the polypeptide $P_i$ with the non-polar ligates	$P$		Standard pressure
		$r^2$		Correlation coefficient
$\eta$	Viscosity of the mobile phase	$R$		Gas constant
$\epsilon_p$	Permeability of the sorbent	RP-HPLC		Reversed phase high performance liquid chromatography
$E$	Internal energy of the polypeptide $P_i$ — non-polar ligates system	$S$		Slope (or gradient) of the plot of $\log k'_i$ vs. $\varphi$ at a defined $T$ in RP-HPLC separations
$F$	Flow rate (ml/min)	$\sigma_{v,i}$		Bandwidth of peak zone
Fmoc-	Fluorenylmethylcarbonyl group	$T$		Temperature in degrees Kelvin
$\varphi$	Volume fraction of organic solvent in a binary water–solvent mixture	$T_{comp}$		Enthalpy–entropy compensation temperature
$\Phi$	Phase ratio of the chromatographic system	$T_{\Delta Cp \rightarrow 0}$		Temperature at which $\Delta C_{p,i}^o \rightarrow 0$
H	Slope of the linearised plot of $\log k'_i$ vs. $1/c_i$ in HPHIC separations	TFA		Trifluoroacetic acid
HPHIC	High performance hydrophobic interaction chromatography	$T_H$		Temperature at which $\Delta H_{assoc,i}^o \rightarrow 0$
HPIEX	High performance ion exchange chromatography	$t_o$		Retention time of a non-interacting solute
HPIMAC	High performance metal ion affinity chromatography	$t_e$		Retention time of a polypeptide $P_i$
$I$	Sum of the change in entropy and the logarithm of the phase ratio, i.e. $(\Delta S_{assoc,i}^o + \ln \Phi)$	$T_S$		Temperature at which $\Delta S_{assoc,i}^o \rightarrow 0$
K	Temperature (degrees Kelvin)	$u$		Linear flow velocity of the eluent ( $= L/t_o$ )
$K_{assoc,i}$	Equilibrium association constant	$U$		Change in a particular parameter or quantity describing the association of the polypeptide $P_i$ with the sorbent
$\kappa^e$	Solvophobic cavity factor related to the ratio in energy re-	$V$		Standard volume
		$Z$		Slope of the linearised plot of $\ln k'_i$ vs. $1/c_i$ in HPIEX separations
		2D-NMR		2-Dimensional nuclear magnetic resonance

## Acknowledgements

These investigations were supported by the Australian Research Council. Dr Michael McLeish and Dr Susan Charman are thanked for providing access to the CD spectropolarimeter whilst Phillip Holt is thanked for assistance with the amino acid analysis.

## References

- [1] M.T.W. Hearn, in: J.C. Janson, L. Ryden (Eds.), *Protein Purification, Principles, High Resolution Methods and Applications*, V.C.H. Press, New York, 1998, pp. 239–282.
- [2] M.I. Aguilar, M.T.W. Hearn, *Meth. Enzymol.* 270 (1996) 1–25.
- [3] E. Lazoura, I. Maidonis, E. Bayer, M.T.W. Hearn, M.I. Aguilar, *Biophys. J.* 72 (1997) 232–246.
- [4] C.T. Mant, R.S. Hodges, in: C.T. Mant, R.S. Hodges (Eds.), *High Performance Liquid Chromatography of Peptides and Proteins: Separation, Analysis and Conformation*, CRC Press, Boca Raton, FL, 1991, pp. 589–658.
- [5] S. Rothmund, E. Krause, M. Beyermann, M. Dathe, H. Engelhardt, M. Bienert, *J. Chromatogr.* 689 (1995) 219–226.
- [6] M.T.W. Hearn, in: C.T. Mant, R.S. Hodges (Eds.), *High Performance Liquid Chromatography of Peptides and Proteins: Separation, Analysis and Conformation*, CRC Press, Boca Raton, FL, 1991, pp. 95–104.
- [7] M.T.W. Hearn, M.I. Aguilar, in: A. Neuberger, L.L.M. Van Deenen (Eds.), *Modern Physical Methods in Biochemistry*, Elsevier Publ., Amsterdam, 1988, pp. 107–142.
- [8] R.I. Boysen, M.T.W. Hearn, in: K.M. Gooding, F.E. Regnier (Eds.), *HPLC of Biological Macromolecules*, Marcel Dekker, New York, 1999, in press.
- [9] F.W. Fang, M.I. Aguilar, M.T.W. Hearn, *Chromatography* 729 (1996) 49–66.
- [10] F.E. Regnier, R.M. Chiciz, in: K.M. Gooding, F.E. Regnier (Eds.), *HPLC of Biological Macromolecules*, Marcel Dekker, New York, 1990, pp. 77–94.
- [11] M.T.W. Hearn, in: M.A. Vijayalakshmi (Ed.), *Theory and Practice of Biochromatography*, Harwood Academic Publishers, Switzerland, 1999, in press.
- [12] S.E. Blondelle, K. Buttner, R.A. Houghten, *J. Chromatogr.* 625 (1992) 199–206.
- [13] R.S. Hodges, P.D. Semchuk, A.K. Taneja, C.M. Kay, J.M.R. Parker, C.T. Mant, *Pept. Res.* 1 (1988) 19–30.
- [14] A.W. Purcell, M.I. Aguilar, M.T.W. Hearn, *Anal. Chem.* 65 (1993) 3038–3047.
- [15] A.W. Purcell, M.I. Aguilar, M.T.W. Hearn, *J. Chromatogr.* 593 (1992) 103–117.
- [16] E. Krause, M. Beyermann, M. Dathe, S. Rothmund, M. Biernert, *Anal. Chem.* 67 (1995) 252–258.
- [17] R.I. Boysen, Y. Wang, M.T.W. Hearn, *J. Pept. Res.*, 1999, submitted.
- [18] M.T.W. Hearn, R.I. Boysen, Y. Wang, S. Muraledaram, in: Y. Shimonishi (Ed.), *Peptide Science*, Kluwer Academic Publishers, 1998, 1–896.
- [19] M.T.W. Hearn, G. Zhao, *Anal. Chem.*, 1998, submitted.
- [20] A.W. Purcell, G. Zhao, M.I. Aguilar, M.T.W. Hearn, *J. Chromatogr.*, 1999, submitted.
- [21] M. Goodman, M. Chorev, *Acc. Chem. Res.* 12 (1979) 1–7.
- [22] M. Chorev, M. Goodman, *Acc. Chem. Res.* 26 (1993) 266–273.
- [23] J.L. Fauchère, C. Thureau, *Adv. Drug. Res.* 23 (1992) 127–159.
- [24] W.M. Kazmierski, R.D. Ferguson, R.J. Knapp, G.K. Lui, H.L. Yamamura, V.J. Hruby, *Int. J. Pept. Protein Res.* 39 (1992) 401–414.
- [25] M. Marraud, V. Dupont, V. Grand, S. Zerkout, A. Lecoq, G. Boussard, J. Vidal, A. Collet, A. Aubry, *Biopolymers* 33 (1993) 1135–1148.
- [26] R.A. Wiley, D.H. Rich, *Med. Res. Rev.* 13 (1993) 327–384.
- [27] M.M. Schemyakin, Yu.A. Ovchinnikov, V.T. Ivanov, A.V. Evstranov, *Nature* 213 (1967) 412–414.
- [28] M.M. Schemyakin, Yu.A. Ovchinnikov, V.T. Ivanov, *Angew. Chem. Int. Ed. Engl.* 8 (1969) 492–498.
- [29] M. Chorev, M. Goodman, *Trends Biotechnol.* 13 (1995) 438–445.
- [30] P.J. Fisher, F.G. Prendergast, M.R. Ehrhardt, J.L. Urbauer, A.J. Wand, S.S. Sedarous, D.J. McCormick, P.J. Buckley, *Nature* 368 (1994) 651–653.
- [31] S. Muller, G. Guichard, N. Benkirane, F. Brown, M.H.V. van Regenmortel, J.-P. Briand, *Pept. Res.* 8 (1995) 138–144.
- [32] G. Guichard, N. Benkirane, G. Zeder-Lutz, G.M.H.V. van Regenmortel, J.-P. Briand, S. Muller, *Proc. Natl. Acad. Sci. USA* 91 (1994) 9765–9769.
- [33] T. Yamazaki, D.F. Mierke, O.E. Said-Nejad, E.R. Felder, M. Goodman, *Int. J. Pept. Protein Res.* 39 (1992) 161–181.
- [34] K.A. Higgins, W. Bicknell, H.H. Keah, M.T.W. Hearn, *J. Pept. Res.* 50 (1997) 421–435.
- [35] H.H. Keah, E. Kecorius, M.T.W. Hearn, *J. Pept. Res.* 51 (1998) 2–11.
- [36] P.L. Privalov, S.J. Gill, *Adv. Protein Chem.* 39 (1988) 191–235.
- [37] K.P. Murphy, P.L. Privalov, S.J. Gill, *Science* 247 (1990) 903–906.
- [38] J.E. Macnair, K.C. Lewis, J.W. Jorgenson, *Anal. Chem.* 69 (1997) 983–989.
- [39] K. Lan, J.W. Jorgenson, *Anal. Chem.* 70 (1998) 2773–2782.
- [40] K.S. Yun, C. Zhu, J.F. Parcher, *Anal. Chem.* 67 (1995) 613–619.
- [41] M.D. Foster, R.E. Synovec, *Anal. Chem.* 68 (1995) 2838–2844.
- [42] K.A. Dill, *J. Phys. Chem.* 91 (1987) 1980–1986.

- [43] L.C. Tan, P.W. Carr, *J. Chromatogr.* 656 (1993) 521–535.
- [44] J.F. Parcher, M.I. Selim, *Anal. Chem.* 51 (1979) 2154–2156.
- [45] J.H. Knox, R.J. Kaliszan, *J. Chromatogr.* 349 (1985) 211–234.
- [46] A. Vailaya, Cs. Horvath, *Ind. Eng. Chem. Res.* 35 (1996) 2964–2982.
- [47] D. Haidacher, A. Vailaya, Cs. Horvath, *Proc. Natl. Acad. Sci. USA* 93 (1996) 2290–2295.
- [48] L.A. Cole, J.G. Dorsey, K.A. Dill, *Anal. Chem.* 64 (1992) 1324–1329.
- [49] E.D. Katz, K. Ogan, R.P.W. Scott, *Anal. Chem.* 352 (1986) 67–75.
- [50] E.D. Katz, C.H. Lochmuller, R.P.W. Scott, *Anal. Chem.* 61 (1989) 349–356.
- [51] K.A. Dill, *Biochemistry* 29 (1990) 7133–7155.
- [52] B. Lee, *Proc. Natl. Acad. Sci. USA* 88 (1991) 5154–5159.
- [53] J. Leffler, E. Grundwald, *Rates and Equilibria of Organic Reactions*, Wiley Interscience, New York, NY, 1963, p. 128.
- [54] R. Lumry, S. Rajender, *Biopolymers* 9 (1970) 1125–1131.
- [55] K.P. Murphy, E. Freire, *Adv. Protein Chem.* 43 (1992) 313–361.
- [56] P.L. Privalov, G.I. Makhatadze, *J. Mol. Biol.* 213 (1992) 385–395.
- [57] T. Vogler, R. Kurth, S. Norley, *J. Immunol.* 153 (1994) 1895–1904.